Non-Shilnikov cascades of spikes and hubs in a semiconductor laser with optoelectronic feedback

Joana G. Freire[1,2] and Jason A. C. Gallas[1,2,3]
[1]*Instituto de Física, Universidade Federal do Rio Grande do Sul, 91501-970 Porto Alegre, RS , Brazil*
[2]*Centro de Estruturas Lineares e Combinatórias, Faculdade de Ciências, Universidade de Lisboa, Lisboa, Portugal*
[3]*Departamento de Física, Universidade Federal da Paraíba, 58051-970 João Pessoa, PB, Brazil*
(Received 5 May 2010; published 21 September 2010)

Incomplete homoclinic scenarios were recently measured in a semiconductor laser with optoelectronic feedback. We show here that such a laser contains cascades of spirals of periodic oscillations and hubs which look identical to the familiar ones observed in *complete* homoclinic scenarios. This means that hubs are far more general than presumed so far, being not limited by Shilnikov's theorem. Laser hubs open the possibility of measuring complex distributions of non-Shilnikov laser oscillations, and we briefly discuss how to do it.

DOI: 10.1103/PhysRevE.82.037202 PACS number(s): 05.45.Pq, 42.65.Sf, 42.55.Ah

An outstanding phenomenon attracting continued attention over the years is the bursting, or spiking, produced by excitable systems as diverse as, for example, the cells responsible for electric activity and insulin production in the pancreatic β cells [1], the cells responsible for vital neurological rhythmicity [2], mixed-mode oscillations of chemical systems [3–5], and all sorts of intensity spiking observed in laser systems [6]. Indeed, one of the very first experimental characteristics studied continuously since the successful operation of the first ruby laser, which commemorates 50 years now [7], was the complicated behaviors displayed by trains of relaxation oscillations consisting of many irregular light spikes [8]. Nowadays, semiconductor lasers are ideal tools to study the intricacies of spiking and chaotic dynamics. For a recent comprehensive review, see Wieczorek *et al.* [6]. The impact of optoelectronic systems in the science and applications of chaos was recently reviewed by Larger and Dudley [9].

Typically, excitable systems are characterized by stable steady states that may be forced to spike by relatively small perturbations above some threshold. They involve multiple-time-scale dynamics [10]. Low-dimensional systems normally display such behavior near Hopf bifurcations, when a fixed point becomes unstable in favor of self-sustained stable oscillations. However, considerably richer scenarios are possible in higher-dimensional systems, particularly when period-doubling cascades follow a Hopf bifurcation and subsequent canard explosion, producing alternations of periodic and chaotic oscillations. As the amplitude of the chaotic attractors grows one observes a spiking regime consisting of large pulses separated by irregular time intervals in which the system displays small-amplitude chaotic oscillations. This scenario, reminiscent of Shilnikov's homoclinic chaos despite the fact that no homoclinic connections are involved, has already been observed in chemical models [3,4] and, very recently, in ground-breaking experimental studies of a semiconductor laser with optoelectronic feedback by Al-Naimee *et al.* [11,12]. Such experiments provide new insight concerning semiconductor lasers by showing that they require extending the concept of excitability beyond that familiar to fixed points into the realm of higher-dimensional attractors, as anticipated theoretically [10]. The authors argued their results to be due to an incomplete homoclinic scenario to a saddle focus where no exact homoclinic connection occurs, a very remarkable feature that opens the possibility of exploring experimentally an elusive non-Shilnikov regime [13–18].

On the other hand, recent work has shown the abundant presence of certain accumulation points in parameter space which act like *periodicity hubs* [16,17] in phase diagrams of dissipative flows like the laser at hand. Briefly [18], by suitably tuning parameters along spirals characterized by oscillations with specific wave forms one navigates toward the hub, the focal accumulation point, where it is possible to *commute* from the incoming spiral to an *infinite variety* of outgoing spirals, each one corresponding to a family of characteristic *stable* oscillations, periodic or not (see Fig. 3 below). The situation resembles closely what happens near the poles of the earth, in a classical navigation problem solved by Nunes in 1537, by introducing the key concept of rhumb lines, later translated into "loxodromic spirals," the curves that underlie Mercator's projection [20]. In certain situations the accumulation hubs are known to be directly linked to Shilnikov's homoclinic scenario [13–16,18], but so far it is totally unclear whether or not hubs exist in more general setups like, here, in semiconductor lasers with optoelectronic feedback displaying incomplete homoclinic scenarios. Although detailed phase diagrams of *chaotic* phases are known for several lasers [21,23], no laser is presently known to display hubs of any kind, with or without Shilnikov's scenario.

The purpose of this Brief Report is to report the discovery of infinite cascades of spirals and periodicity hubs [16–18] in the control (parameter) space of the semiconductor laser with ac-coupled optoelectronic feedback of Al-Naimee *et al.* [11,12]. This finding is relevant because no hubs, remarkable dynamical objects still in their infancy, are presently known for any laser. In addition, the laser hub presently found is *not* of the "standard" type spotted so far, which has its local dynamics ruled by Shilnikov's theorem [13–15,18]. According to Al-Naimee *et al.* [11,12], semiconductor lasers with optoelectronic feedback provide an example of a non-Shilnikov scenario, which are shown here to contain a profusion of spirals and hubs. Such hubs open now the possibility of probing experimentally intricate and unexplored dynamics in a domain where essentially everything still remains to be investigated both theoretically and experimentally (for applications, see the last paragraph).

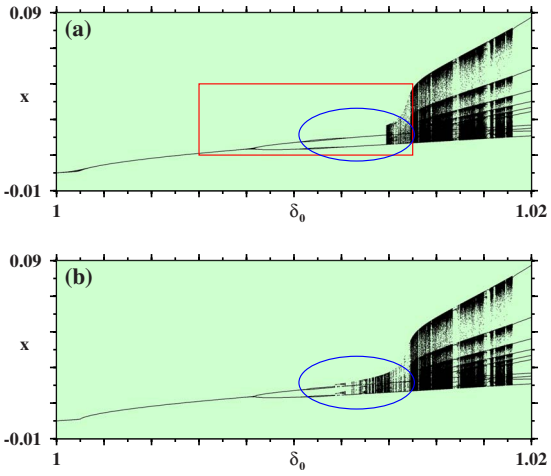

FIG. 1. (Color online) Multistable laser operation evidenced by bifurcations dependent on initial conditions. Ellipses mark the region where multistability is easily recognizable. (a) Bifurcations obtained when starting integrations always from the same (arbitrary) initial condition $(x_0,y_0,w_0)=(1,1.5,0.5)$. The box indicates the region studied by Al-Naimee *et al.* [11] (see their Fig. 4). (b) Bifurcations obtained when "following the attractor" [19] horizontally from left to right, starting from $(x_0,y_0,w_0)=(1,1.5,0.5)$. Here, $\varepsilon=2\times10^{-5}$.

Using parameters related directly with experimental quantities, the dimensionless semiconductor laser model is [11,12]

$$\frac{dx}{dt}=x(y-1), \tag{1}$$

$$\frac{dy}{dt}=\gamma[\delta_0-y+f(w+x)-xy], \tag{2}$$

$$\frac{dw}{dt}=-\varepsilon(w+x), \tag{3}$$

where the feedback amplifier function is $f(w+x)=\alpha\frac{w+x}{1+s(w+x)}$, α is a coefficient proportional to the photodetector responsivity, γ is the ratio between the population relaxation rate and the photon damping, ε is the high-pass frequency in the feedback loop, δ_0 is the solitary laser threshold, and s is a saturation coefficient of the amplifier [11,12]. These are suitably scaled free parameters. The variable x is proportional to the photon density, y is proportional to the carrier density, and w is proportional to the intensity. Following Refs. [11,12], we fix $\alpha=1$, $\gamma=0.001$, $s=11$ and investigate the dynamics as a function of δ_0, the solitary laser threshold, and ε, the high-pass frequency in the feedback loop. Phase diagrams were obtained by computing the full Lyapunov spectra for Eqs. (1)–(3) using a standard fourth-order Runge-Kutta algorithm with a fixed time step $h=0.05$. The first 10^7 time steps were discarded as transient; the Lyapunov spectrum was computed during the subsequent 3×10^7 steps [18]. As a first result, Fig. 1 illustrates wide ranges of multistability in the laser operation by displaying bifurcation diagrams of the maxima of x obtained in the two traditional ways of dealing with initial conditions, as described in the caption.

Motivated by the work of Al-Naimee *et al.* [11,12] we investigated in more detail the same parameter regions accessible to their experiments. Figure 2 shows phase diagrams obtained by discretizing a grid of parameters and, for each point of the grid, discriminating between periodic oscillations (plotted as black dots) and chaos (plotted as white dots). A total of $1200\times1200\simeq1.4\times10^6$ Lyapunov exponents are displayed in each panel in Figs. 2 and 3. The boxes in Fig. 2(a) indicate the location of two of the largest spiral nestings and hubs seen in this parameter range. The boxes are shown magnified in Figs. 2(b) and 2(c). Additional magnifications (not shown) reveal an infinity of similar spirals and hubs.

Figure 3 is intended to illustrate with greater detail the regular organization typically observed locally around individual hubs. Every dark spiral is formed by an infinite sequence of stable laser oscillations with a specific wave form. Wave forms evolve continuously as one spirals inward toward the focal accumulation point. Concomitantly, the period of the oscillations grows without limit, diverging at the accumulation point. It is important to realize that the focal point is an *asymptotic* limit point that is beyond rigorous

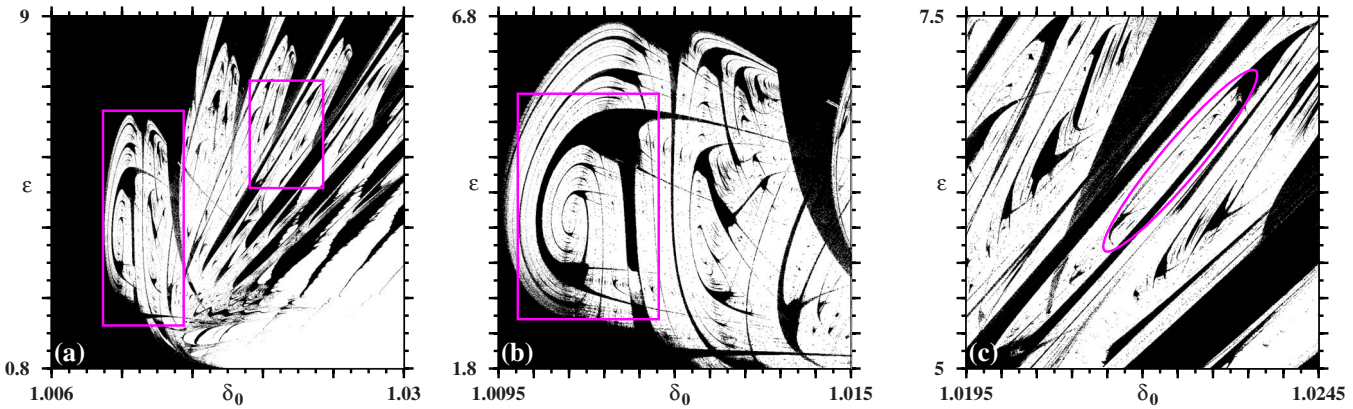

FIG. 2. (Color online) Bichromatic phase diagrams discriminating periodicity (shown in black) from chaos (in white). (a) Global view of parameter space with boxes around the two largest hubs in this region. Chaotic lobes "reverberate" as in a driven Duffing oscillator [22]. (b) Zoom of the leftmost box in (a). The box is magnified in Fig. 3; (c) zoom of the rightmost box in (a) containing hubs and spirals stretched and tilted in the region inside the ellipse. All vertical axes are multiplied by 10^5, i.e., in (a) the axis runs from 0.8×10^{-5} to 9.0×10^{-5}.

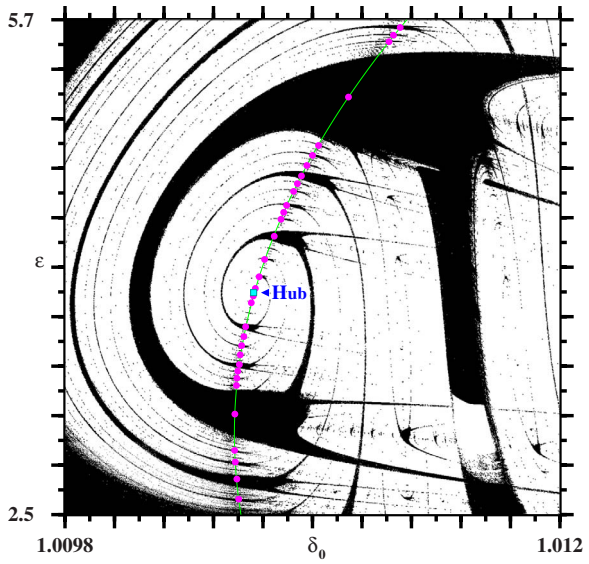

FIG. 3. (Color online) Magnification of the box in Fig. 2(b) displaying the focal hub (the square indicated by the arrowhead), the infinite spirals attached to it, and the characteristic regular parameter organization "induced" by hubs around them. The parabolic curve, defined by Eq. (4), passes through the dots marking shrimp heads (described in Refs. [24,25]). Here, $2.5\times10^{-5}\leq\varepsilon\leq5.7\times10^{-5}$.

reach, much in the same way as Nunes proved the poles of his spherical earth to be totally out of reach of the loxodromics. Of course, experimental resolution (noise) puts a limit on the macroscopic size (observability) of the focal "point." In other words, mathematics has not prevented anyone from reaching the poles.

By least-squares fitting a parabola to the "shrimp heads" [24,25], i.e., to reference points suitably scattered along the spirals, we were able to obtain an approximate equation passing by construction through the "center" of the infinite alternation of windows of periodicity and of chaos. This line corresponds to a *stability locus* of the laser:

$$\delta_0 = 106\ 946\ 0\epsilon^2 - 64.6514\epsilon + 1.011\ 53. \qquad (4)$$

This curve is superimposed in light gray (green online) in Fig. 3, along with dots indicating the shrimp heads used to fit the parabola. The focal hub F is estimated to be near the point

$$F = (\delta_0, \varepsilon) = (1.010\ 639, 3.9355\times10^{-5}). \qquad (5)$$

The laser phase diagram is riddled with an infinite quantity of such stability loci as it is easily recognizable under suitable magnifications.

As it is intuitively clear from Fig. 3, more elaborate bifurcation diagrams obtained by *tuning simultaneously two parameters* along Eq. (4) display an *ordering symmetry* with respect to a reflection about the hub. This symmetry is illustrated in Fig. 4.

How difficult is to record experimentally spirals in phase diagrams like the ones in Figs. 2 and 3? Although our figures were generated by computing Lyapunov exponents, there is

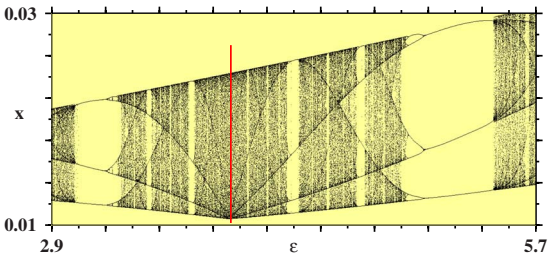

FIG. 4. (Color online) Bifurcation diagram illustrating the reflection symmetry of the window *ordering* about the hub, indicated by the vertical black line (red online). The diagram displays maxima of x observed when tuning ε and δ_0 *simultaneously* along the parabolic curve of Eq. (4), shown in Fig. 3. The hub is located at the minimum of the local maxima of x. Here, $2.9\times10^{-5}\leq\varepsilon\leq5.7\times10^{-5}$.

absolutely no need of computing Lyapunov exponents experimentally to detect spirals. As the bichromatic representation used in our Figs. 2 and 3 shows, all that needs to be done is to use a *pair of colors*, say black and white, to discriminate between two states: periodicity or lack of periodicity, i.e., "chaos." For experimentally obtained time series this might be conveniently achieved in several simple ways. For instance, one may compare successive extrema (maxima or minima) of the signal to detect periodicity and to perform the bichromatic binary selection. Or one may construct return maps and detect periodicity from them. Alternatively, one might measure the "time of flight" among successive maxima or minima of the signal using such measurements to either directly detect periodicity or construct return maps and detect periodicities on the fly [14]. Yet another possibility is to plot the frequencies obtained by Fourier transforming the experimental time series [26]. While a fair experimental resolution of the periodicity certainly improves the overall definition of the phase diagram obtained, simple computer experiments show that even a relatively modest discrimination between period and lack of period is enough to generate good phase diagrams. In this sense, spirals are robust objects. In fact, we conjecture the final resolution of experimentally measured phase diagrams to be much more sensitive to the ability of tuning parameters finely than to the ability of discriminating between the presence and absence of periodicities. The number of spirals detected is certainly limited by experimental resolution (noise) [18].

In conclusion, we identified infinite cascades of hubs as responsible for organizing both periodic and nonperiodic (spiking) laser phases in a semiconductor laser with optoelectronic feedback in which Al-Naimee *et al.* measured recently an incomplete homoclinic scenario to a saddle focus (a system without an exact homoclinic connection). The big surprise here is that, although the semiconductor laser is not operating in a Shilnikov regime, one still finds for it the same hubs presently believed to exist only near saddle foci which obey Shilnikov's theorem. Thus, semiconductor lasers with optoelectronic feedback provide examples of periodicity hubs that are not related to homoclinic bifurcations, as anticipated [16,18]. Of course, the laser is merely a convenient vehicle to describe a novel phenomenon which we conjecture to be not only generic but in fact relatively abundant in

dissipative flows. Understanding the extension and structure of chaotic laser phases is of great interest in chaos-based secure communications [27]. With chaos-enabled random number generators it is expected that the performance of random number generators can be greatly improved with chaotic laser devices as physical entropy sources. Hubs in chaotic lasers are also expected to have an impact in a whole host of next generation rf photonics subsystems such as remote sensors of laser radiation, chaotic radar, laser radar, and optical systems that generate passively diverse arbitrary wave forms where, for example, preliminary experiments based on an optically injected geometry show subcentimeter accuracy in ranging with a 3-cm-range resolution [23,27]. It is remarkable that navigation along spirals in laser phase diagrams turns out to be so similar to the solution found by Nunes many centuries ago to the problem of optimizing navigation: move along rhumb lines, which form infinite families of loxodromic spirals.

Note added. The spirals and hubs anticipated theoretically in Refs. [16,17] were observed experimentally now [28]. As already pointed out [16], we emphasize that while it is tempting to associate periodicity hubs with homoclinic orbits and with a theorem by Shilnikov, numerical work shows hubs and spirals not to exist in several flows that are textbook examples of the Shilnikov scenario [18]. This means that under Shilnikov conditions, spirals and hubs can be either observed or not.

J.G.F. is supported by FCT, Portugal, Grant No. SFRH/BPD/43608/2008 and IF-UFRGS for hospitality. J.A.C.G. is supported by CNPq, Brazil, and by AFOSR Grant No. FA9550-07-1-0102. All computations were done in the clusters of CESUP-UFRGS.

[1] T. R. Chay, J. Theor. Biol. **142**, 305 (1990); D. Hawker and P. Ashwin, Int. J. Bifurcation Chaos **15**, 2819 (2005).

[2] *Bursting: The Genesis of Rhythm in the Nervous System*, edited by S. Coombes and P. Bressloff (World Scientific, Singapore, 2005); J. E. Rubin, Scholarpedia J. **2**, 1666 (2007); E. M. Izhikevich, Int. J. Bifurcation Chaos **10**, 1171 (2000).

[3] V. Petrov, S. K. Scott, and K. Showalter, J. Chem. Phys. **97**, 6191 (1992).

[4] M. T. M. Koper, P. Gaspard, and J. H. Sluyters, J. Chem. Phys. **97**, 8250 (1992).

[5] A. Goryachev, P. Strizhak, and R. Kapral, J. Chem. Phys. **107**, 2881 (1997).

[6] S. Wieczorek, B. Krauskopf, T. B. Simpson, and D. Lenstra, Phys. Rep. **416**, 1 (2005).

[7] T. Maiman, Nature (London) **187**, 493 (1960).

[8] C. L. Tang, H. Statz, and G. deMars, J. Appl. Phys. **34**, 2289 (1963); B. I. Davis and D. V. Keller, Appl. Phys. Lett. **5**, 80 (1964); T. Shimizu *et al.*, Jpn. J. Appl. Phys. **4**, 445 (1965); H. Risken and K. Nummedal, J. Appl. Phys. **39**, 4662 (1968); R. Graham and H. Haken, Z. Phys. **213**, 420 (1968).

[9] L. Larger and J. M. Dudley, Nature (London) **465**, 41 (2010).

[10] F. Marino, F. Marin, S. Balle, and O. Piro, Phys. Rev. Lett. **98**, 074104 (2007); C. K. R. T. Jones and A. I. Khibnik, *Multiple-Time-Scale Dynamical Systems* (Springer, New York, 2000).

[11] K. Al-Naimee, F. Marino, M. Ciszak, R. Meucci, and F. T. Arecchi, New J. Phys. **11**, 073022 (2009).

[12] K. Al-Naimee, F. Marino, M. Ciszak, S. F. Abdalah, R. Meucci, and F. T. Arecchi, Eur. Phys. J. D **58**, 187 (2010).

[13] P. Glendinning, *Stability, Instability and Chaos* (Cambridge University Press, Cambridge, England, 1994); L. A. Belyakov, Math. Notes **15**, 336 (1974); **28**, 910 (1981); P. Glendinning and C. Sparrow, J. Stat. Phys. **35**, 645 (1984); P. Gaspard, R. Kapral, and G. Nicolis, *ibid.* **35**, 697 (1984); F. T. Arecchi, Chaos **1**, 357 (1991).

[14] T. Braun, J. A. Lisboa, and J. A. C. Gallas, Phys. Rev. Lett. **68**, 2770 (1992).

[15] R. Vitolo, P. Glendinning, and J. A. C. Gallas (unpublished).

[16] C. Bonatto and J. A. C. Gallas, Phys. Rev. Lett. **101**, 054101 (2008).

[17] G. M. Ramirez-Avila and J. A. C. Gallas, Rev. Boliviana Fis. **14**, 1 (2008); G. M. Ramirez-Avila, *ibid.* (to be published).

[18] For a survey, see J. A. C. Gallas, Int. J. Bifurcation Chaos **20**, 197 (2010), and references therein.

[19] J. G. Freire, R. J. Field, and J. A. C. Gallas, J. Chem. Phys. **131**, 044105 (2009).

[20] P. Nunes, *Tratado em Defensam da Carta de Marear (Treatise Defending the Sea Chart)*, Obras Vol. I (Gulbenkian, Lisboa, 2002), reprint of the 1537 original; R. D'Hollander, Mare Liberum **1**, 29 (1990); J. Alexander, Math. Mag. **77**, 349 (2004).

[21] C. Bonatto, J. C. Garreau, and J. A. C. Gallas, Phys. Rev. Lett. **95**, 143905 (2005); C. Bonatto and J. A. C. Gallas, Phys. Rev. E **75**, 055204(R) (2007); Philos. Trans. R. Soc. London, Ser. A **366**, 505 (2008).

[22] C. Bonatto, J. A. C. Gallas, and Y. Ueda, Phys. Rev. E **77**, 026217 (2008).

[23] V. Kovanis, A. Gavrielides, and J. A. C. Gallas, Eur. Phys. J. D **58**, 181 (2010).

[24] J. A. C. Gallas, Phys. Rev. Lett. **70**, 2714 (1993); Physica A **202**, 196 (1994); Appl. Phys. B: Lasers Opt. **60**, S203 (1995).

[25] E. N. Lorenz, Physica D **237**, 1689 (2008).

[26] M. Lepers, V. Zehnlé, and J. C. Garreau, Phys. Rev. Lett. **101**, 144103 (2008).

[27] J. M. Liu, in *Semiconductor Laser Dynamics for Novel Applications*, Applications of Nonlinear Dynamics, edited by V. In *et al.* (Springer, Berlin, 2009), and references therein.

[28] R. Stoop, P. Benner, and Y. Uwate, Phys. Rev. Lett. **105**, 074102 (2010); Proceedings of the 18th IEEE Workshop on Nonlinear Dynamics of Electronic Systems (NDES), Dresden, 2010, edited by R. Tetzlaff, W. Schwarz, and K. Kelber (unpublished), pp. 6–9.